

# DEVELOPMENT AND APPLICATION OF MODIFIED FUEL PERFORMANCE CODE BASED ON STAINLESS STEEL AS CLADDING UNDER STEADY STATE, TRANSIENT AND ACCIDENT CONDITIONS

ALFREDO ABE\*, ANTONIO TEIXEIRA E SILVA\*, CLAUDIA GIOVEDI+, CAIO MELO+, DANIEL DE SOUZA GOMES\*, RAFAEL RONDON MUNIZ+

\*Instituto de Pesquisas Energéticas e Nucleares - IPEN/CNEN-BRAZIL

Avenida Prof. Lineu Prestes 2242, Cidade Universitária – São Paulo – Brazil.

+ Escola Politécnica – Universidade de São Paulo LABRISCO

Avenida Prof. Mello Moraes 2231, Cidade Universitária – São Paulo – Brazil.

## Abstract

The IPEN/CNEN proposal for FUMAC-CRP was to modified fuel performance codes (FRAPCON and FRAPTRAN) in order to assess the behavior of fuel rod using stainless steel as cladding and compare to zircaloy cladding performance under steady state and accident condition. The IFA 650-9, IFA-650-10 and UFA-650-11 experiments were modelled to perform the LOCA accident simulation considering the original cladding and compared to stainless steel cladding.

## 1. INTRODUCTION

The nuclear fuel behaviour under accidental conditions is a main concern during the fuel design process, especially for safety analysis. In particular, the most challenging design basis accidents (DBA) such as loss of coolant accident (LOCA) and reactivity initiated accident (RIA) have been investigated experimentally in order to quantify properly the safety criteria associated to the fuel rod and those experiments allow the verification of capabilities of fuel performance codes. The FUMAC CRP is aiming at analysis of fuel behaviour under normal and off normal condition considering the capabilities of fuel performance code to simulate the experiments dedicated to LOCA accident condition. Several set of LOCA experimental data were made available to the participants in order to address different fuel parameters by means of codes simulations, furthermore some sensitivity and uncertainties analysis were addressed. The IPEN/CNEN proposal for FUMAC-CRP was to investigate the stainless steel cladding performance under same conditions as zircaloy cladding fuel. The comparison could contribute to verify the stainless steel cladding performance under accident condition.

## 2. ACTIVITIES PERFORMED

The CRP initial activities start with introductory studies and literature surveys associated to the LOCA accident such as phenomena, license safety criteria, experiments performed, simulation of accident using several codes and their results [1]–[9]. The initial activities performed illustrate how challenging is the analysis of LOCA accident and still open issues associated to the fuel performance codes to reproduce adequately the experimental results. The following activities had been performed at first year of CRP:

- Experiments data and description made available were evaluated in order to select the most appropriated experiments for simulation;
- Experimental data were proper retrieved from selected experiment data file;
- FRAPCON [10] and FRAPTRAN [11] codes input data and modelling were addressed;
- Simulation of selected experiments using original version of FRAPCON and FRAPTRAN codes were performed;
- Preliminary results evaluation and analysis were carried out;
- FRAPCON and FRAPTRAN codes were modified in order to consider stainless steel as cladding material;

- Initial verification of implemented modification in FRAPCON and FRAPTRAN codes were performed;
- Simulations of selected experiments using modified version (stainless steel cladding) of FRAPCON and FRAPTRAN were conducted, and;
- Preliminary results evaluation and comparison with zircaloy cladding were performed.

Those activities listed above were conducted during 2015/2016 and some obtained results were presented at 2nd RCM Meeting. At final phase (2016/2017) of the CRP, following activities were conducted:

- FRAPTRAN subroutine modification,
- Sensitivity and Uncertainties assessment, and
- Obtained results compilation and analysis.

Those activities were conducted during 2016/2017 and obtained results will be presented at 3rd RCM Meeting.

## 2.1. Experimental Data Assessment and Codes Simulation

The experimental data of LOCA experiments were made available to the participants of the CRP with additional HWR reports (Halden Technical Report) and Data Sheet Description. The selected experimental data are from IFA-650.9, IFA-650.10 and IFA50.11 experiments, and all data were retrieved from experimental data files and plotted (see Fig. 1 to 8) in order to verify the behaviour and trends.

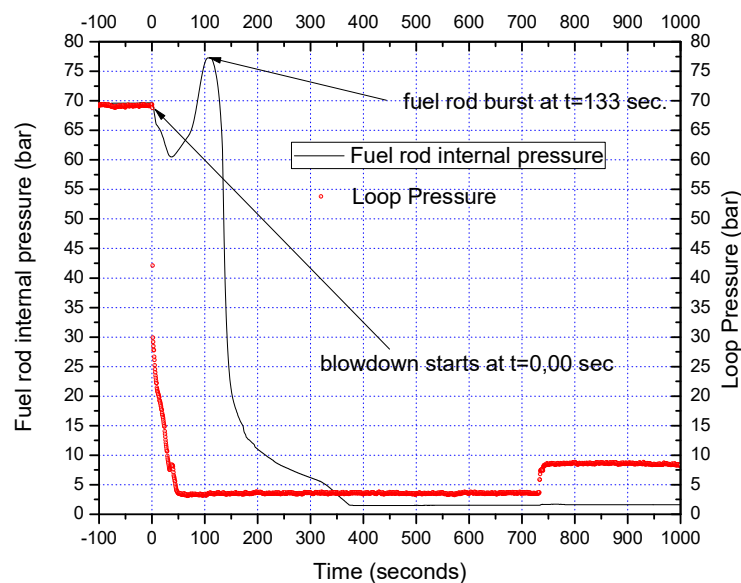


FIG. 1. Experimental data (loop and fuel internal pressure) from IFA-650.9.

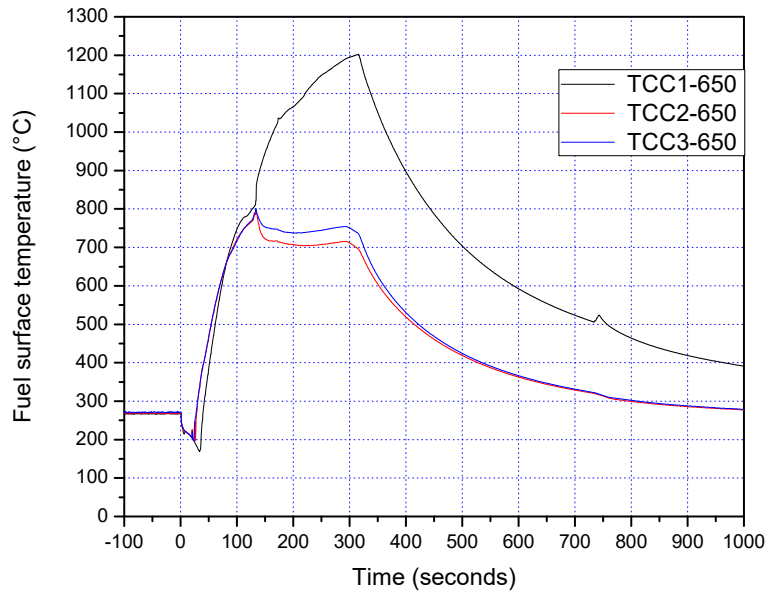


FIG. 2. Experimental data (Thermocouple) from IFA-650.9.

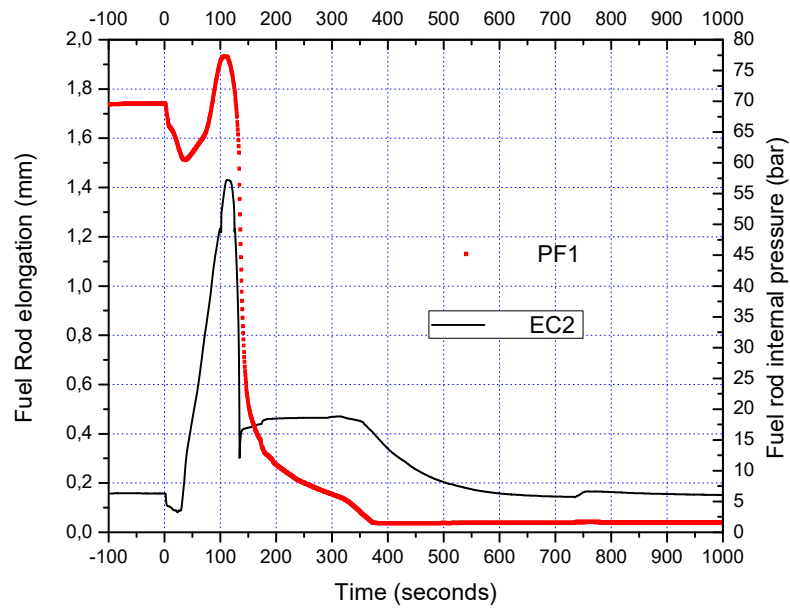


FIG. 3. Experimental data (Fuel internal pressure and clad elongation) from IFA-650.9.

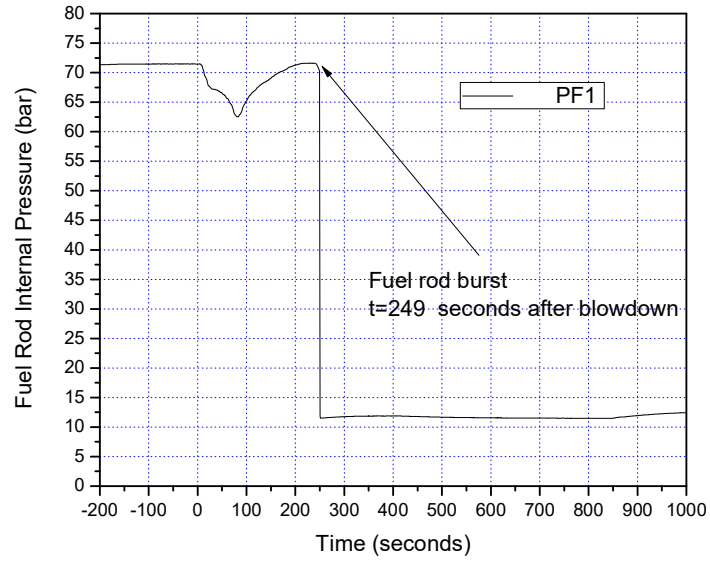


FIG. 4. Experimental data (Fuel internal pressure) from IFA-650.10.

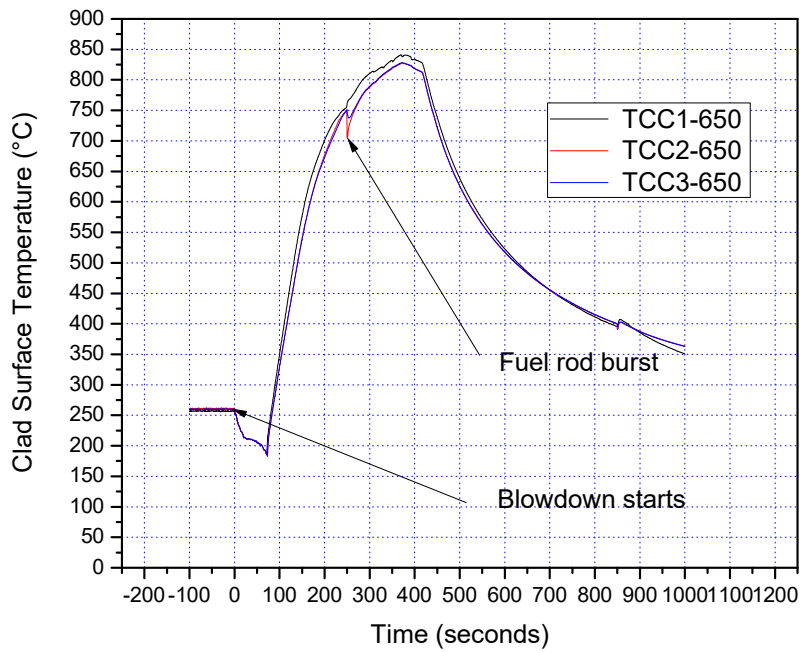


FIG. 5. Experimental data (Thermocouple) from IFA-650.10.

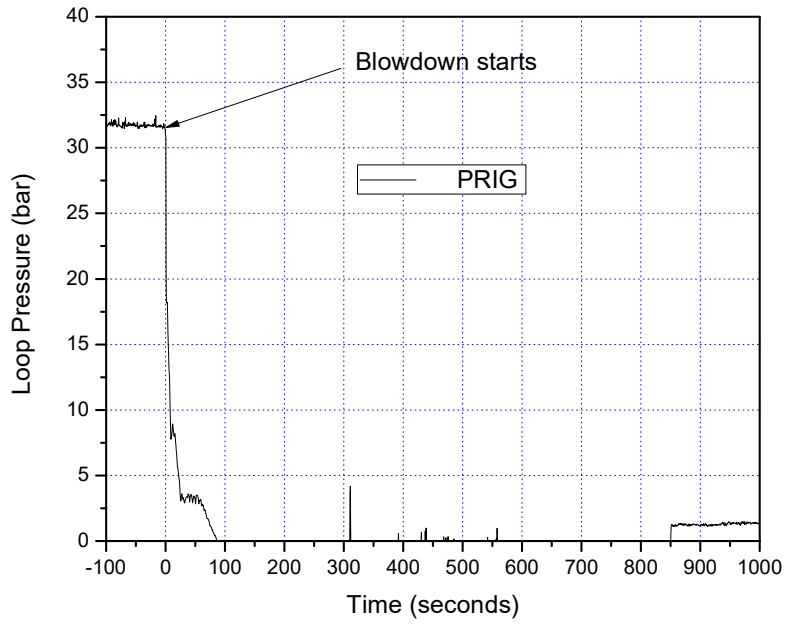


FIG. 6. Experimental data (Loop Pressure) from IFA-650.10.

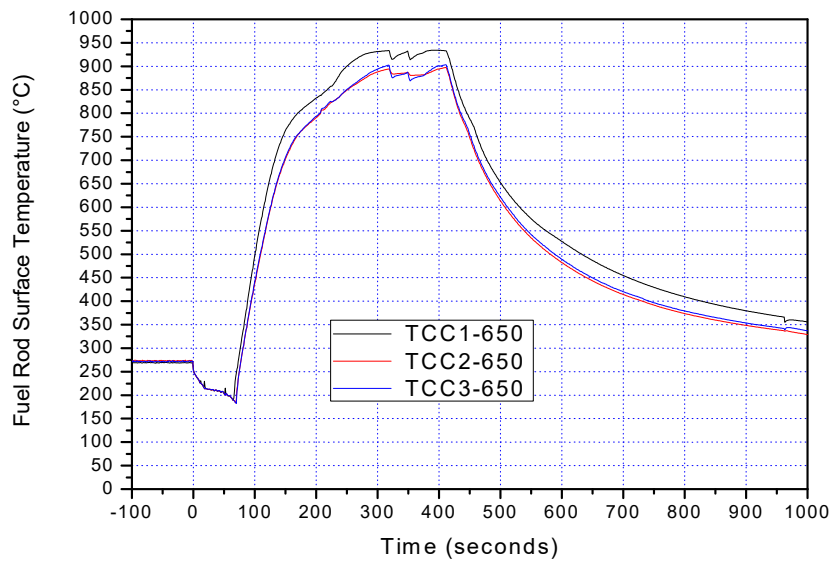


FIG. 7. Experimental data (Thermocouple) from IFA-650.11.

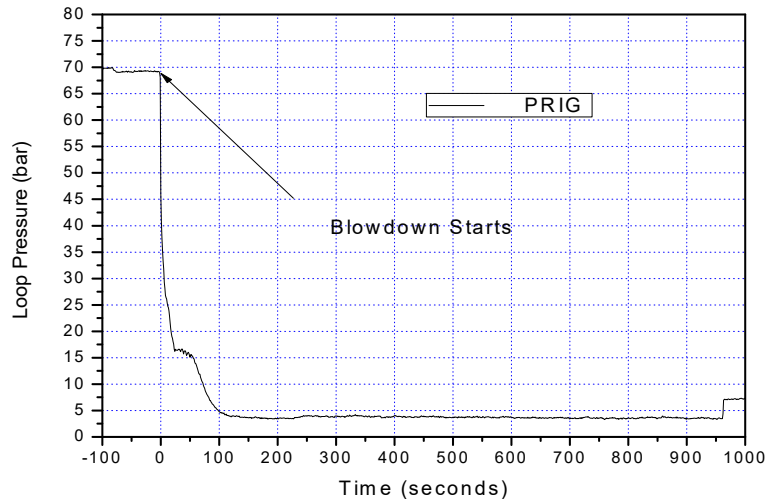


FIG. 8. Experimental data (Loop Pressure) from IFA-650.11.

The input data for FRAPCON and FRAPTRAN codes were prepared using information available from the technical reports made available.

The FRAPCON code required data as fuel geometry, composition and irradiation condition (power profile) were taken from HALDEN Data Sheet QA-F-702 and HWR-917 technical reports for the experiment IFA-650.09.

The FRAPCON code required data as fuel geometry, composition and irradiation condition were taken from HALDEN Data Sheet IFA-650.10 and HWR-974 technical reports for the experiment IFA-650.10.

The FRAPCON code required data as fuel geometry, composition and irradiation condition were taken from HALDEN Data Sheet IFA-650.11 and HWR-976 technical reports for the experiment IFA-650.11.

## 2.2. Preliminary results for Zircaloy cladding

The base irradiation (burnup accumulation) simulations using FRAPCON code (original version) were performed in order to address some fuel parameters (fission gas release, temperature, pressure, hoop stress, etc.) related to base irradiation. Additionally, the FRAPCON simulation creates an initialization file to be utilized in the FRAPTRAN calculation (LOCA simulation). As example of some results obtained from FRAPCON code (base irradiation), the following Figs 9, 10 and 11 present the fuel centerline temperature as function of burnup level obtained for base irradiation of IFA-650.09, IFA-650.10 and IFA-650.11 cases.

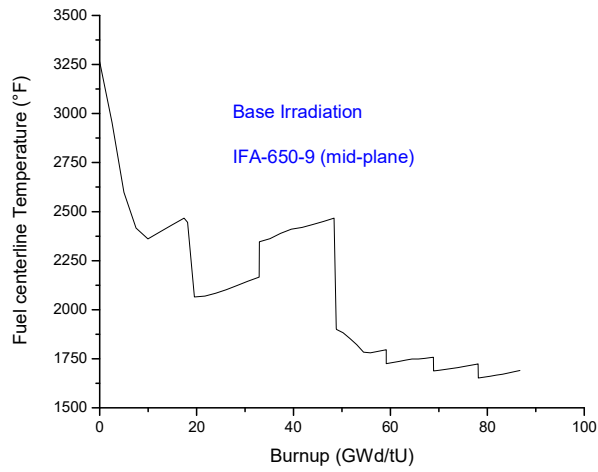


FIG. 9. Fuel Centerline as function of Burnup (IFA-650.09).

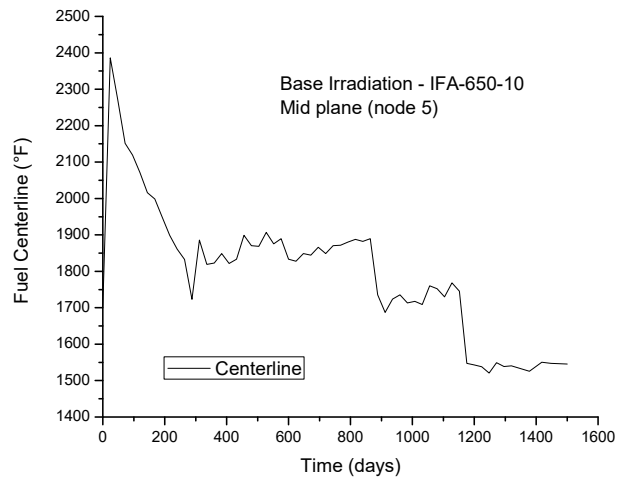


FIG. 10. Fuel Centerline as function of Burnup (IFA-650.10).

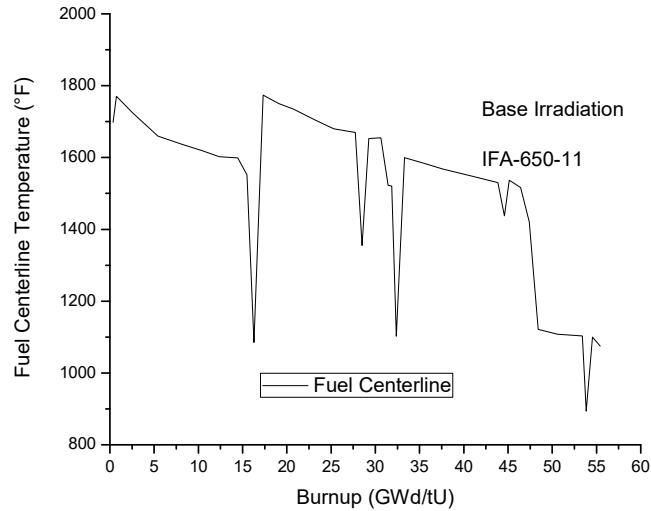


FIG. 11. Fuel Centerline as function of Burnup (IFA-650.11).

Others fuel parameters such as internal pressure evolution, fission gas release fraction (%), plenum gas temperature, clad temperature profile, gap thickness, clad strain, hoop stress, and others were also evaluated for each IFA case, and those results were presented at 2° RCM.

The transient/accident simulations were performed using FRAPTRAN code (original version), which is an analytical code applied to calculate fuel rod behaviour when power or coolant boundary conditions, or both, are changing quite fast. The FRAPTRAN code calculates power, fuel and cladding temperatures, cladding elastic and plastic stress and strain, cladding oxidation, and fuel rod gas pressure as function of time. The fuel parameters that are slowly varying with time (burnup), such as fuel densification and swelling, and cladding creep and irradiation growth are not calculated by FRAPTRAN code. Those parameters are read from a file generated by FRAPCON code during the steady state simulation.

All required input data were taken from same technical reports already mentioned before. Additional required data (temperature and pressure as function of time) were taken from experimental data file.

The time length for LOCA experiment simulation (IFA series) was considered 100 s before the blowdown phase and up to reactor SCRAM, so the fuel rod burst time was properly considered, others input data were prepared according to FRAPTRAN User's Manual.

As example of obtained results from FRAPTRAN code, the following Fig. 12 to 14 present the fuel rod pressure evolution during the LOCA for IFA-650.09, IFA-650.10 and IFA-650.11 cases, respectively.



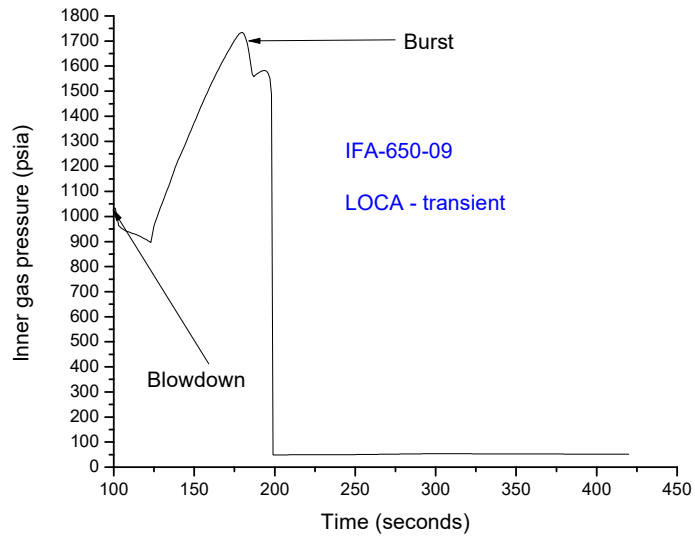


FIG. 12. Inner gas pressure during the LOCA simulation (IFA-650.09).

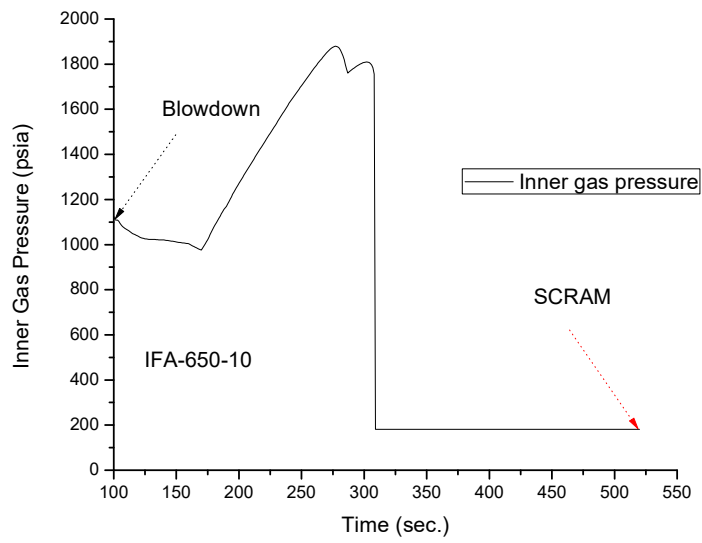


FIG. 13. Inner gas pressure during the LOCA simulation (IFA-650.10).

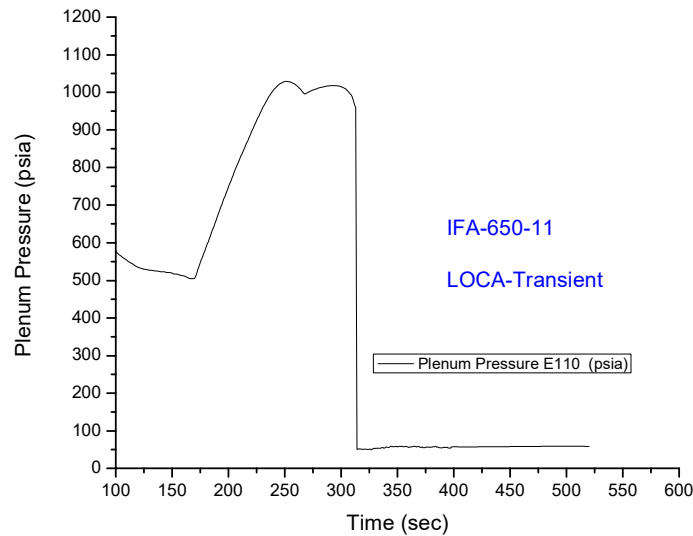


FIG. 14. Plenum gas pressure during the LOCA simulation (IFA-650.11).

### 2.3. FRAPCON and FRAPTRAN codes modification for stainless steel cladding

The IPEN contribution for FUMAC-CRP was to perform assessment and analysis considering stainless steel as cladding material. After Fukushima Daiichi nuclear accident, the ATF (Accident Tolerant Fuel) became a very important issue. In this context, the IPEN/CNEN (Brazil) has presented a proposal to modify the FRAPCON/FRAPTRAN codes in order to consider iron (Fe) based alloys as cladding material. Originally, FRAPCON/FRAPTRAN codes consider only zirconium based alloys as cladding material (Zircaloy-2, Zircaloy-4, M5, Zirlo, Improved Zirlo, and E110).

Existing material properties in the FRAPCON code was considered in modular subroutines that define material properties (thermal and mechanical) for temperatures ranging from room temperature to temperatures above melting and for fuel rod-average burnup levels between 0 and 62 gigawatt-days per metric ton of uranium. Each subroutine defines only a single material property: fuel thermal conductivity as a function of fuel temperature, fuel density, and burnup; fuel thermal expansion as a function of fuel temperature; and the cladding stress-strain relation as a function of cladding temperature, strain rate, cold work, hydride content, and fast neutron fluence.

In order to perform modification properly, initially all subroutines related to material properties were clearly identified. After verification of existing information in the specific subroutine related to material properties, the modification was performed replacing zirconium alloy data for stainless steel data. Some material properties for stainless steel were not available in the open literature, in that case, the material properties were not changed at all. Additional details can be found in the reference [12]: Revisiting Stainless Steel as PWR Fuel Rod Cladding after Fukushima Daiichi Accident, published in Journal of Energy and Power Engineering 8 (2014).

Some qualitative and quantitative comparisons were performed in other to verify the modifications implemented in the FRAPCON (stainless steel version) code. The FRAPTRAN code modification approach was the same as FRAPCON code and the verification was in process at that time (2016).

Specifically, for IFA experiment series simulations, the mechanical properties related to hoop strain and stress of cladding were not changed, due to that, the cladding burst failure should not be reliable and revision was planned for the future simulation (third year).

According to FRAPTRAN code documentation (User Manual), the BALON2 subroutine calculates the extent and shape of the localized large cladding deformation that occurs between the time that the cladding effective strain exceeds the instability strain and the time of cladding rupture. The BALON2 model predicts failure in the ballooning node when the cladding true hoop stress exceeds an empirical limit that is a function of temperature. The empirical limit was not changed in this work due to lack of burst data for iron based alloys. The limit adopted in this work was taken from the FRAPTRAN – User’s Manual, specifically the Fig. 2.18 (True hoop stress at burst as function of temperature).

## 2.4. Preliminary results for Stainless Steel cladding

The obtained results from FRAPCON/FRAPTRAN modified version were compared to original version of both codes (FRAPCON and FRAPTRAN) for zirconium based alloy.

The preliminary results are presented in Table 1 (base irradiation) and Table 2 (LOCA condition).

The base irradiation has shown similar results, main difference should be associated to heat transfer coefficient (zirconium alloy and Fe alloy). The material property difference cause an increase of fuel pellet temperature and high fission gas release, consequently slightly high internal fuel rod pressure.

TABLE 1. BASE IRRADIATION RESULTS FROM FRAPCON (ORIGINAL VERSION) AND FRAP-SS-IPEN (MODIFIED VERSION FOR AISI-348)

Parameters	IFA-650.09		IFA-650.10		IFA-650.11	
	Zircaloy	Stainless Steel	Zircaloy	Stainless Steel	E110	Stainless Steel
Maximum rod internal pressure (PSIA)	1376	1390	1231	1231	645	631
Fission gas release (%)	13.81	14.13	0.16	2.35	1.94	1.94
Maximum fuel centerline temperature (°F)	3267	3293	2397	2534	1782	1845

The result (see Table 2) obtained for LOCA simulation, somehow were not in good agreement due to ballooning (maximum circumferential strain data), the IFA-650.10 results for stainless steel were higher than zirconium alloy, others cases (IFA-650.09 and IFA-650.11) exhibited different trend. The mechanical ballooning model in the FRAPTRAN (BALON2) was not modified for the stainless steel code version due to that, the results are not consistent as expected. The assessment of ballooning model for stainless steel was in progress at that time.

TABLE 2. LOCA-TRANSIENT RESULTS FROM FRAPTRAN (ORIGINAL VERSION) AND FRAP-SS-IPEN (MODIFIED VERSION FOR AISI-348)

Parameters	IFA-650.09		IFA-650.10		IFA-650.11	
	Zircaloy	Stainless Steel	Zircaloy	Stainless Steel	E110	Stainless Steel
Burst (sec)	99	134	109	110	258	267
Rod burst at elevation (ft)	0.787	0.787	0.722	0.722	0.787	0.787
Clad ballooning - maximum circumferential strain (%)	31.25	30.58	74.66	87.71	38.83	30.94

TABLE 2. LOCA-TRANSIENT RESULTS FROM FRAPTRAN (ORIGINAL VERSION) AND FRAPT-SS-IPEN (MODIFIED VERSION FOR AISI-348)

Parameters	IFA-650.09		IFA-650.10		IFA-650.11	
	Zircaloy	Stainless Steel	Zircaloy	Stainless Steel	E110	Stainless Steel
plenum gas pressure (PSIA)	48.68	49.73	181.4	181.4	58.15	56.62
plenum gas temperature (F)	1333	1476	1282	1284	1581	1599

Figures 15 to 17 present internal pressure evolution during the LOCA accident, obtained considering iron alloy and zirconium alloy for IFA-650.9, IFA-650.10, and IFA-650.11, respectively.

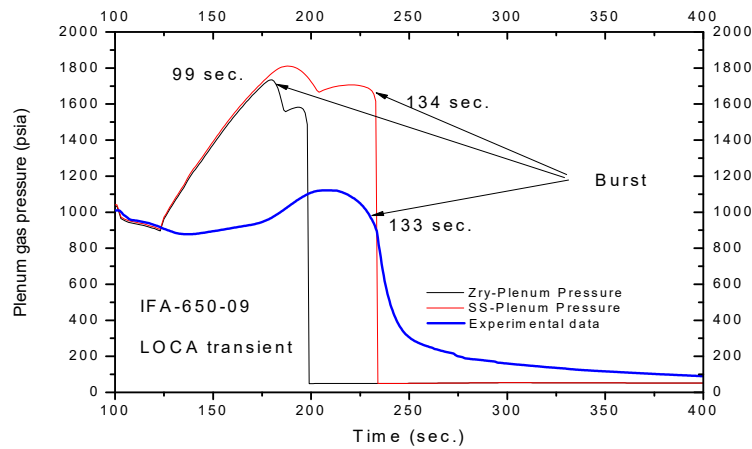


FIG. 15. Internal pressure evolution (plenum) during the LOCA transient (IFA-650.09).

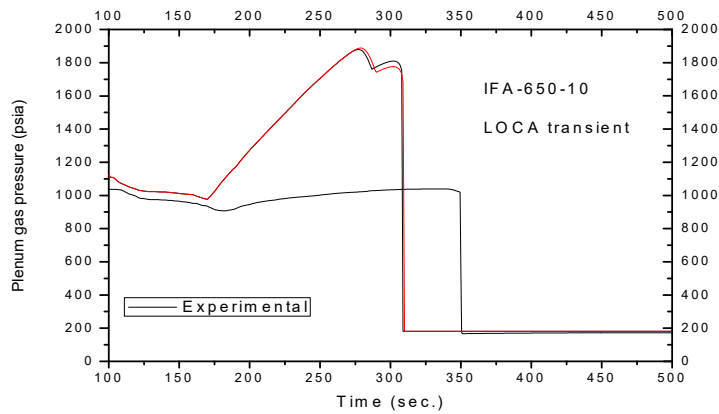


FIG. 16. Internal pressure evolution (plenum) during the LOCA transient (IFA-650.10).

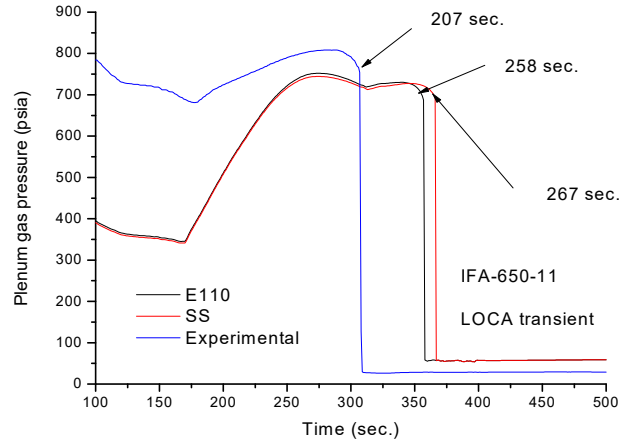


FIG. 17. Internal pressure evolution (plenum) during the LOCA transient (IFA-650.11).

According to recent publication: Cladding burst behavior of Fe-based alloys under LOCA [13], the stainless steel (Fe alloy) hoop stress parameter as function of temperature is higher than zirconium alloy (Fig. 4 of mentioned publication).

The mechanical model related to ballooning was detailed investigated in order to modify properly the subroutines associated to the burst calculations.

## 2.5. Review of FRAPCON and FRAPTRAN codes modification for stainless steel Cladding

The results obtained from the FRAPTRAN code modification and additional information from literature shown clearly that results might not be consistent. In order to verify better the burst phenomena, the subroutines dedicated to burst were verified in deep.

Considering that, the FRAPTRAN code shares with FRAPCON some subroutines related to the cladding, part of the modifications already implemented in the modified version of FRAPCON code for AISI 348 (stainless steel), could be utilized to change the FRAPTRAN code. Then, the modification of FRAPTRAN was reviewed step by step, initially the following subroutines from FRAPCON code were used in the FRAPTRAN: CCP, CELMOD, CSHEAR, CMHARD, CTHEXP, CTHCON, ZOEMIS, and ZOTCON. The subroutines related to mechanical properties of cladding such as stress and strain evaluation during the transient of cladding were identified in the CMLIMIT [14] and CKMN subroutines, which calculate the limits of mechanical strain and the plastic strain for the cladding, respectively.

The modification was performed introducing in the code the data related to the burst stress as function of temperature for AISI-304 (stainless steel) obtained from Ref. [13], according to the equation 1:

$$ctstrt = (599.98 - 0.73269 \cdot T_c + 0.0002143 \cdot T_c^2) \cdot 10^6 \quad (1)$$

where:

$ctstrt$  is the tangential component of real stress at burst (in Pa);  
 $T_c$  is the temperature (in °C).

The stress-strain behavior in the FRAPTRAN code is described using two different correlations based on stress [8]. The deformation in the elastic region is described by the Hooke's law as shown in equation 2:

$$\sigma = E\varepsilon \quad (2)$$

where:

- $\sigma$  is the stress;
- $E$  is the modulus of elasticity; and
- $\varepsilon$  is the strain.

The elastic strain is described by a power law

$$\sigma = K\varepsilon^n \left(\frac{\dot{\varepsilon}}{10^{-3}}\right)^m \quad (3)$$

where:

- $K$  is the strength coefficient;
- $n$  is the strain hardening exponent;
- $m$  is the strain rate sensitivity constant; and
- $\dot{\varepsilon}$  is the strain rate.

From Eqs (2) and (3) was obtained the stress-strain curve with yield strength (YS), ultimate tensile strength (UTS), and uniform elongation (EU) for the studied material.

The coefficient  $K$  and the exponent  $n$  in equation 3 as function of temperature for stainless steel were obtained from Ref. [15].

The value for the constant  $m$  was not available for stainless steel, the  $m$  value was kept the same of the zircaloy, considering that the open literature shows that  $m$  values for metals are about 0.1 to 0.2. Those modifications were implemented and a verification of the modified version was performed using another LOCA experiment (IFA-650.5). The obtained results have shown qualitatively a better agreement with expected for stainless steel. Furthermore, IFA-650-10 experiment was verified and compared to previous modification, where the elasto-plastic deformation was not properly addressed; it is clearly that modification implemented represent better the deformation (Fig. 19).

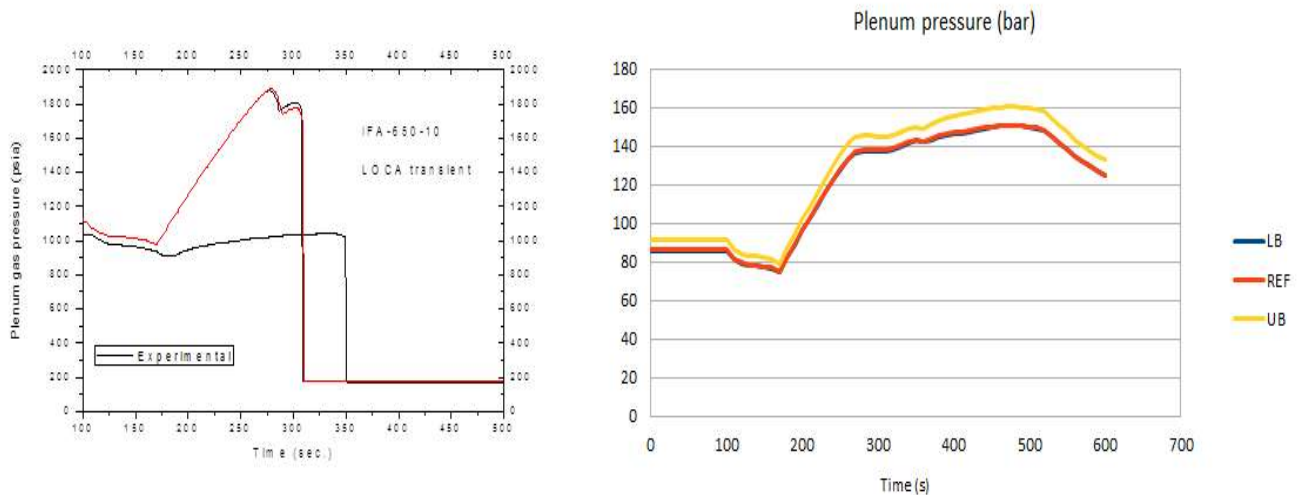


FIG. 18. Plenum pressure (IFA-650-10) evolution, left picture represent preliminary results before elasto-plastic implementation in the FRAPTRAN, right picture is after elasto-plastic properties of stainless steel implement in the FRAPTRAN.

## **2.6. Sensitivity and Uncertainties Assessment and Analysis for IFA-650.10 Considering Zircaloy and stainless steel cladding**

The uncertainty and sensitivity assessment was conducted mostly according to Technical Specification (see Annex I). The IPEN/CNEN approach to perform the sensitivity analysis was slightly different compared to Technical Specification, mainly EXCEL spreadsheet was considered as a tool to assist in statistical analysis instead of DAKOTA package. The statistical distribution (normal) was applied for each one of the fuel fabrication/design parameters and for fuel models (physical properties) utilized in the fuel performance code (FRAPCON) models. The coupled (FRAPCON and FRAPTRAN) simulation was performed by means of script (GNU-OCTAVE), where all inputs files were generated and the results from outputs files were extracted automatically. The obtained results were statistically treated using EXCEL spreadsheet (Pearson Correlation) and some transient results were gathered in standard spreadsheet format as suggested by Dr. J. Zhang. The codes FRAPCON and FRAPTRAN applied to perform the assessment were the original version (as released by NRC for zirconium alloy) and a modified version (including material properties of AISI-348 cladding).

The IFA-650.10 experiment was modelled properly for steady state condition (FRAPCON) and transient (FRAPTRAN) condition taking into account the experimental data (temperature and pressure profile). Thermo-hydraulics calculation data from SOCRATES code were not considered.

Initially, a set of simulations was performed considering 200 (two hundred) runs (FRAPCON and FRAPTRAN), where fuel fabrication/design parameters were considered, such as: cladding thickness, gap thickness, fuel pellet outside diameter,  $U^{235}$  enrichment, fuel theoretical density and rod gas-gap fill pressure. The statistical distribution (normal) and tolerance interval (upper and lower bounds) for each fuel fabrication/design parameter were considered as suggested in the Technical Specification. Additionally, following fuel models (physical properties) embedded in the FRAPCON code were addressed: fuel thermal conductivity, fuel thermal expansion coefficient, cladding axial growth model, cladding creep model, fuel swelling model, fission gas release model, cladding corrosion and, cladding hydrogen pickup. The statistical distribution (normal) was considered as well as correspondent standard deviation for each fuel model (physical properties) as suggested in the Technical Specification. Moreover, suggested uncertainties in the boundary condition were not addressed because only the experimental data were taken into account for modelling the transient simulation. As the irradiation conditions (steady state) are explicitly simulated, the uncertainties in the initial states of the fuel rod will be propagated from steady state to transient simulation.

The IFA-650.10 experiment was addressed also considering stainless steel as cladding material and all others data were not changed, including irradiation condition and transient boundary condition.

After all simulations, the main outcomes are Pearson Correlation and some specific behavior and trends presented in the set of curves. Some extract of results presented in the Technical Report of sensitivity and uncertainties assessments are presented below.

TABLE 3. PEARSON CORRELATION FOR EACH FUEL FABRICATION PARAMETER FOR IFA-650.10.

Fabrication/design tolerance	Fission gas release	Maximum Plenum pressure	Peak fuel centerline temperature
dco	-0.02	0.10	-0.07
thkclad	0.01	0.01	-0.50
thkgap	0.28	0.13	0.99
enrch	0.05	0.08	-0.02
den	-0.87	-0.19	-0.04
fgpav	0.12	0.94	-0.15

\*200 cases (normal distribution)

Table 3 shows the results obtained from FRAPCON (original version) considering the fuel fabrication parameters: cladding thickness (thkclad), gap thickness (thkgap), fuel pellet outside diameter (dco), U<sup>235</sup> enrichment (enrch), fuel theoretical density (den), rod gas-gap fill pressure (fgpav). The results have shown that there are three strong Pearson correlation related to fuel fabrication parameters, as can be seen for fuel density and fission gas release, fuel rod fill gas pressure and maximum plenum pressure, gap thickness and fuel centerline temperature. The Pearson correlation outcome agrees with the expected results. As gap thickness increases, the heat transfer from fuel surface to clad surface will be degraded, consequently the fuel centerline temperature will increase. The higher initial fill rod gas pressure will produce higher final plenum pressure.

The following fuel model uncertainty parameters were addressed: fuel thermal conductivity (sigftc), fuel thermal expansion coefficient (sigftex), cladding axial growth (siggro), cladding creep (sigcreep), fuel swelling (sigswell), fission gas release (sigfgr), cladding corrosion (sigcor) and cladding hydrogen pickup (sigh2). Table 4 shows the results of Pearson Correlation due to the fuel models.

TABLE 4. PEARSON CORRELATION FOR EACH FUEL MODEL FOR IFA-650.10.

Fuel model	Fission gas release	Maximum Plenum pressure	Peak fuel centerline temperature
sigftc	NA	0.03	-0.55
sigftex	NA	0.04	-0.84
sigfgr	NA	0.07	-0.04
sigswell	NA	0.02	0.03
sigcreep	NA	-0.11	-0.07
siggro	NA	-0.10	-0.04
sigcor	NA	-0.04	0.17
sigh2	NA	-0.95	0.00

\*200 cases (normal distribution)

It can be seen from Table 4, that there are three strong Pearson Correlation (PRC > 5.0) related to fuel model as can be seen for fuel thermal expansion coefficient, fuel thermal conductivity and, cladding hydrogen pickup, all correlations are negative.

The initial assessment have shown as each set of parameters (fuel fabrication and fuel model) are correlated taking into account isolated contribution and combination. The fuel fabrication parameters are more strong correlated to final results in the steady state simulation. As steady state condition at the end of irradiation somehow will propagate to transient simulation, it can be expected that, existing correlation somehow will contribute to the transient results.



After steady state simulations, transient simulations were addressed considering combined approach (fuel fabrication and fuel model) uncertainties due to the finding obtained in the first assessment (steady state simulation). According to Technical, the transient simulation results should be selected at specific phenomena time window in order to verify the existing correlation with the input parameters. The results selected to verify the correlation are related to thermal and mechanical behavior of fuel and cladding: Plenum Pressure, Fuel Centerline Temperature, Fuel Surface Temperature, Cladding Inner Temperature, Cladding Outer Temperature, Cladding Hoop Strain, Cladding Effective Stress, Cladding Radial Strain, Cladding Axial Elongation, Fuel Stack Elongation, Fuel Energy, and Fuel Surface Displacement. The phenomena time windows are: beginning of blowdown (100 s), end of blowdown (110 s), before burst (300 s), after burst (320 s) and, end of simulation (600 s).

The following tables (Tables 5, 6 and 7) present the Pearson Correlation results at beginning of blowdown.

TABLE 5. PEARSON CORRELATION\* FOR TRANSIENT SIMULATION AT BEGINNING OF BLOWDOWN (T=100 S) FOR IFA-650.10.

Parameter	Plenum Pressure	Fuel Center Temperature	Fuel Surface Temperature	Clad Inner Temperature
dco	0.12	-0.08	-0.07	-0.02
thkcld	0.44	0.06	0.05	0.04
thkgap	-1.00	0.28	0.22	-0.03
enrch	-0.02	0.79	-0.20	0.33
den	-0.03	-0.47	-0.46	0.36
fgpav	0.11	0.16	0.12	-0.01
sigftc	-0.03	0.04	-0.03	0.02
sigftex	-0.03	0.00	-0.01	0.00
sigfgr	-0.11	0.00	0.05	0.03
sigswell	-0.07	-0.01	0.03	0.02
sigcreep	-0.02	0.04	0.00	0.03
siggro	-0.08	0.04	0.10	0.02
sigcor	0.02	0.01	-0.02	0.12
sigh2	-0.05	0.07	0.00	-0.02

\*Nomenclature:

High correlation (grey color):  $PRC > 0.50$  (absolute value)

Medium correlation (yellow color):  $0.25 < PRC < 0.50$  (absolute value)

Low correlation (white color):  $PRC < 0.25$  (absolute value)

TABLE 6. PEARSON CORRELATION\* FOR TRANSIENT SIMULATION AT BEGINNING OF BLOWDOWN (T=100 S) FOR IFA-650.10.

Parameter	Cladding Outer Temperature	Cladding Hoop Strain	Cladding Effective Stress	Cladding radial Strain
dco	0.00	-0.12	-0.12	0.12
thkcld	0.00	-0.44	-0.44	0.44
thkgap	0.00	1.00	1.00	-1.00
enrch	0.00	0.02	0.02	-0.03
den	0.00	0.03	0.04	-0.03
fgpav	0.00	-0.11	-0.11	0.11

TABLE 6. PEARSON CORRELATION\* FOR TRANSIENT SIMULATION AT BEGINNING OF BLOWDOWN (T=100 S) FOR IFA-650.10.

Parameter	Cladding Outer Temperature	Cladding Hoop Strain	Cladding Effective Stress	Cladding radial Strain
sigftc	0.00	0.03	-0.01	-0.03
sigftex	0.00	0.03	-0.01	-0.03
sigfgr	0.00	0.11	0.07	-0.11
sigswell	0.00	0.07	0.02	-0.08
sigcreep	0.00	0.02	-0.03	-0.02
siggro	0.00	0.08	0.03	-0.08
sigcor	0.00	-0.02	-0.06	0.02
sigh2	0.00	0.05	0.03	-0.06

\*Nomenclature:

High correlation (grey color):  $PRC > 0.50$  (absolute value)

Medium correlation (yellow color):  $0.25 < PRC < 0.50$  (absolute value)

Low correlation (white color):  $PRC < 0.25$  (absolute value)

TABLE 7. PEARSON CORRELATION\* FOR TRANSIENT SIMULATION AT BEGINNING OF BLOWDOWN (T=100 S) FOR IFA-650.10.

Parameter	Cladding Axial Elongation	Fuel Stack Elongation	Fuel energy	Fuel Surface Displacement
dco	-0.08	-0.08	-0.05	-0.12
thkeld	0.06	0.06	0.09	-0.44
thkgap	0.28	0.28	0.33	1.00
enrch	0.79	0.79	0.46	0.03
den	-0.48	-0.48	-0.73	0.03
fgpav	0.16	0.16	0.17	-0.11
sigftc	0.05	0.05	0.03	0.03
sigftex	0.00	0.00	-0.02	0.03
sigfgr	0.00	0.00	-0.01	0.11
sigswell	-0.01	-0.01	-0.01	0.07
sigcreep	0.04	0.04	0.03	0.02
siggro	0.04	0.04	0.05	0.08
sigcor	0.02	0.02	0.02	-0.02
sigh2	0.07	0.07	0.05	0.05

\*Nomenclature:

High correlation (grey color):  $PRC > 0.50$  (absolute value)

Medium correlation (yellow color):  $0.25 < PRC < 0.50$  (absolute value)

Low correlation (white color):  $PRC < 0.25$  (absolute value)

The following Figs 19 to 24 present the trend curves considering reference case (RF) bounding by lower (LB) and upper (UB) limits. Those Figures are also presented in the specific Technical Report regarding sensitivity and uncertainties assessment.

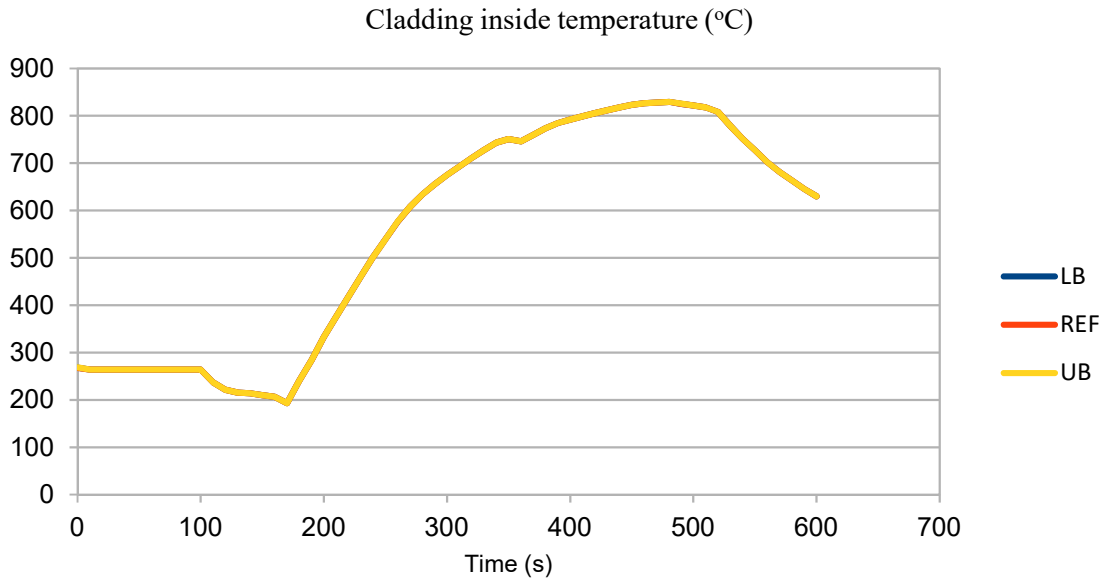


FIG. 19. Cladding inside temperature profile during the transient.

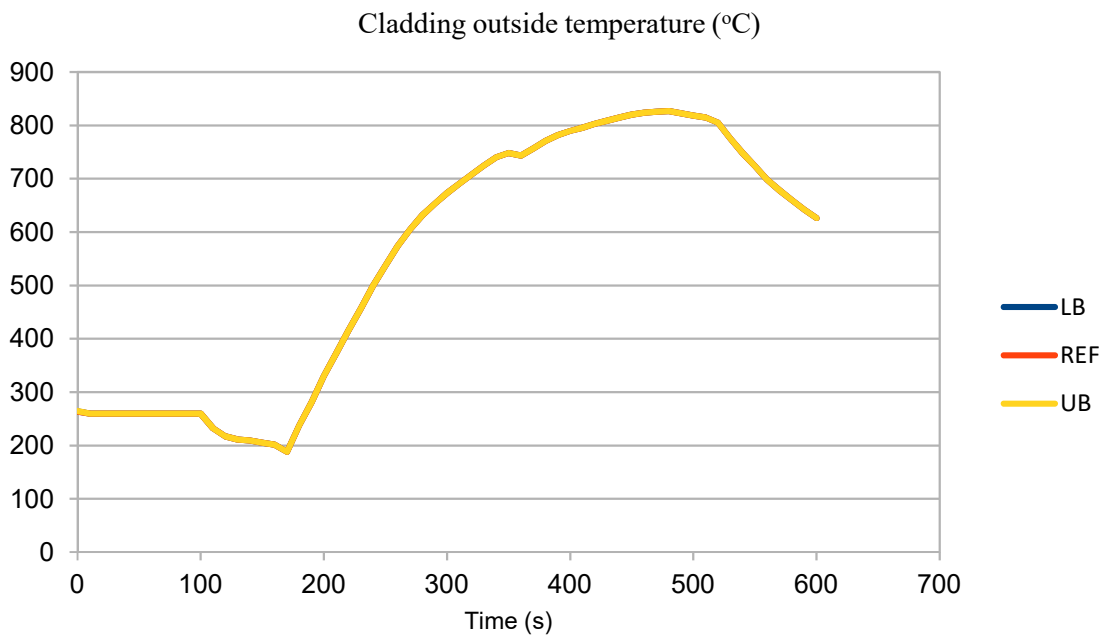


FIG. 20. Cladding outside temperature profile during the transient.

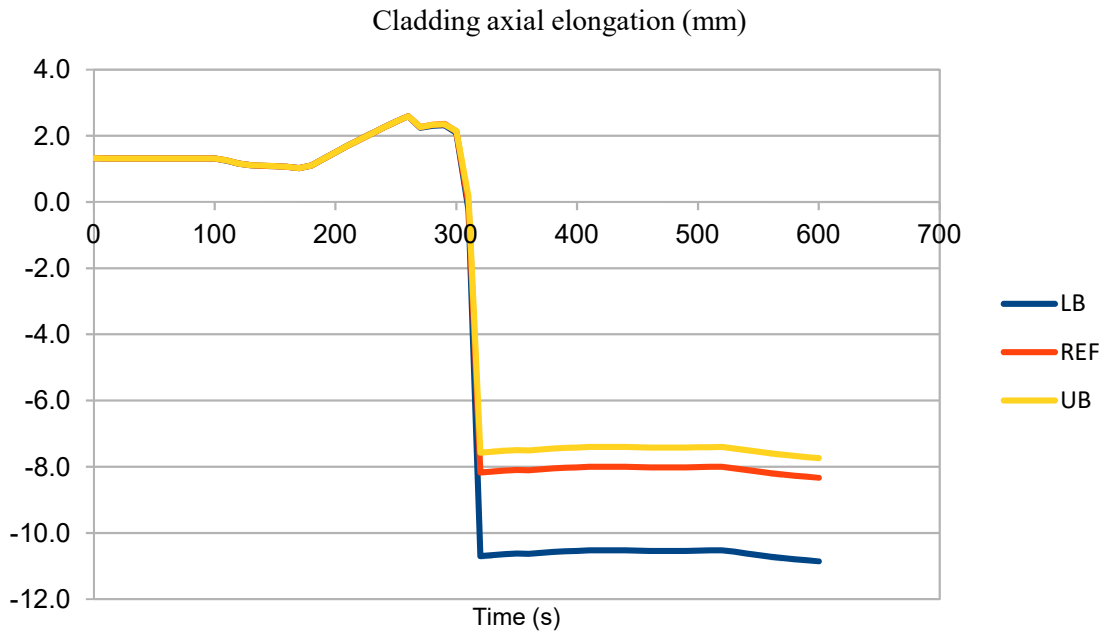


FIG. 21. Cladding axial elongation during the transient.

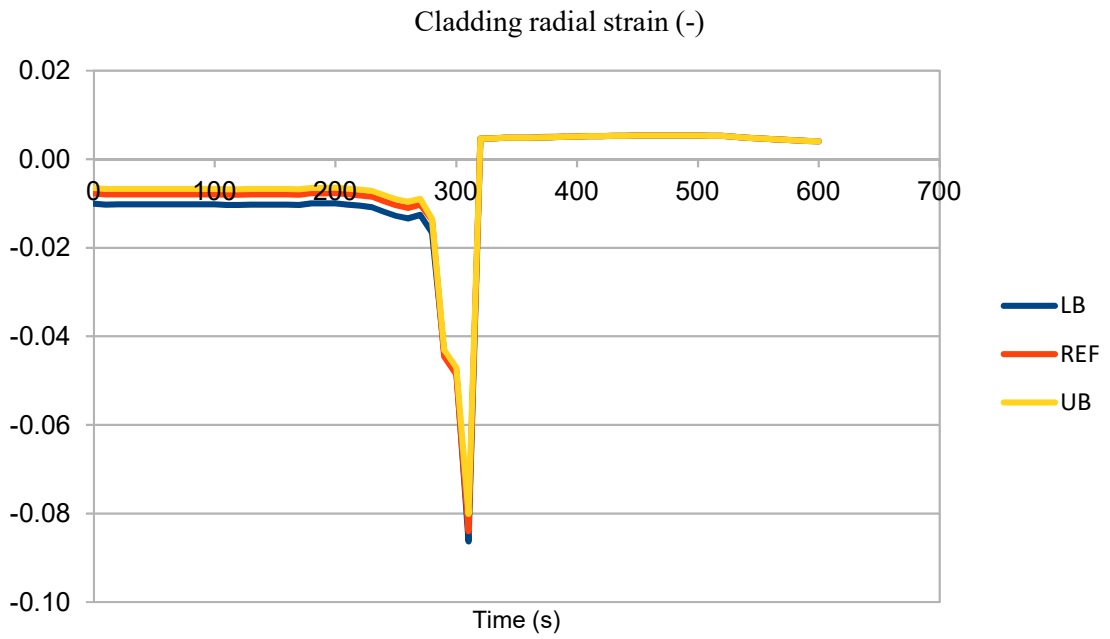


FIG. 22. Cladding radial strain during the transient.

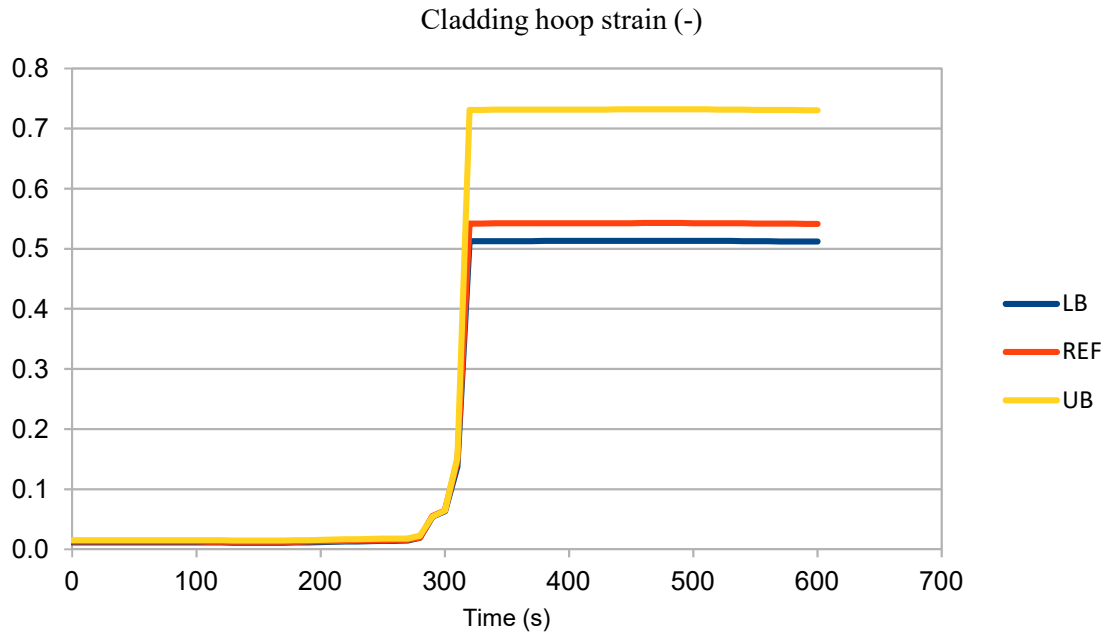


FIG. 23. Cladding hoop strain during the transient.

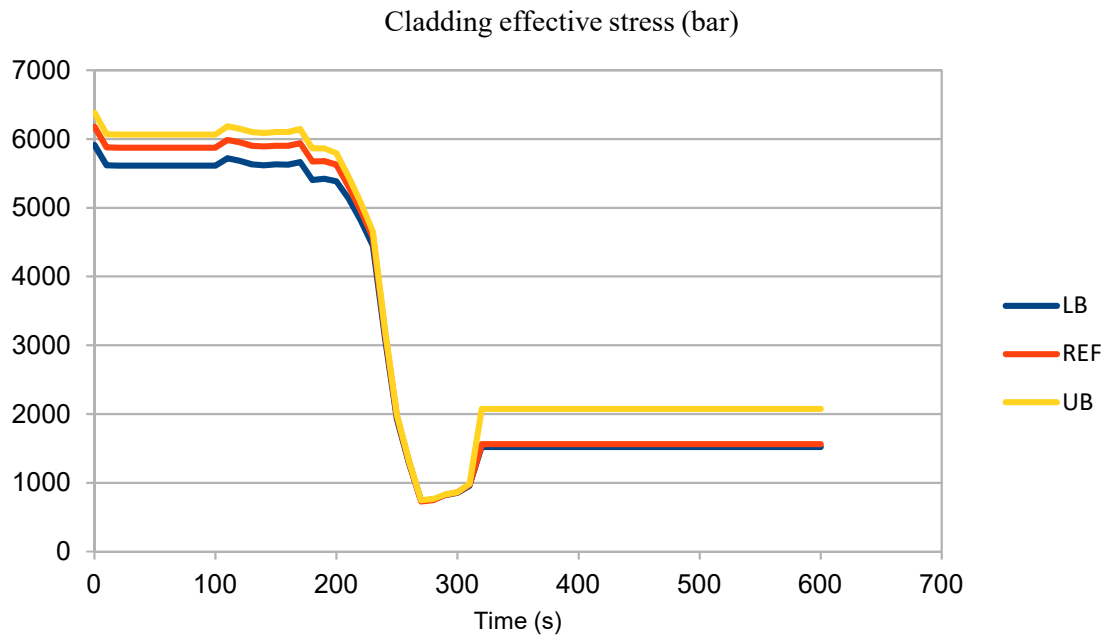


FIG. 24. Cladding effective stress during the transient.

The stainless steel assessment was carried out using the same approach as zircaloy cladding. Only the fuel cladding material was changed in the modelling, all others fuel data and boundary conditions were kept as original IFA-650.10. As example, Table 8 presents the results (Person Correlation) obtained for stainless steel.

TABLE 8. PEARSON CORRELATION FOR EACH FUEL FABRICATION PARAMETER AND FUEL MODEL (STAINLESS STEEL AS CLADDING).

Fuel model and fuel fabrication tolerance	Fission gas release	Maximum plenum pressure	Peak fuel centerline temperature
dco	-0.10	-0.01	-0.08
thkcld	-0.52	-0.35	-0.50
thkgap	0.98	0.78	0.97
enrch	-0.02	0.04	-0.02
den	-0.03	-0.15	-0.08
fgpav	-0.18	0.45	-0.14

\*200 cases (normal distribution)

The following Figs. 25 to 30 present the trend curves obtained for stainless steel cladding considering reference case (RF) bounding by lower (LB) and upper (UB) limits for each one of the transient results selected for analysis. Those Figures were taken from specific Technical Report (already delivered) of Sensitivity and Uncertainties Assessment.

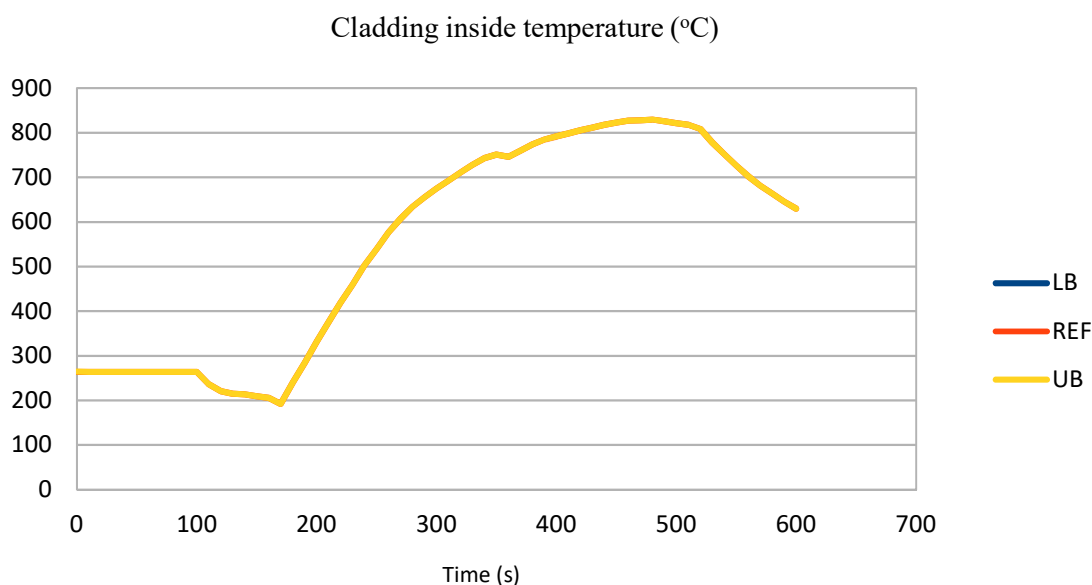


FIG. 25. Cladding (stainless steel) inside temperature profile during the transient.

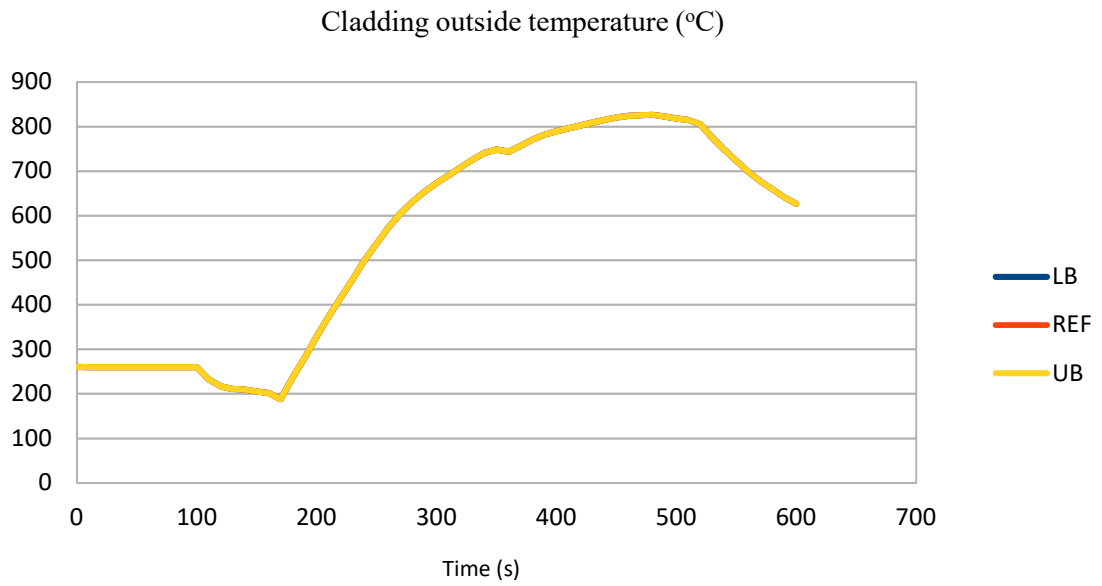


FIG. 26. Cladding (stainless steel) outside temperature profile during the transient.

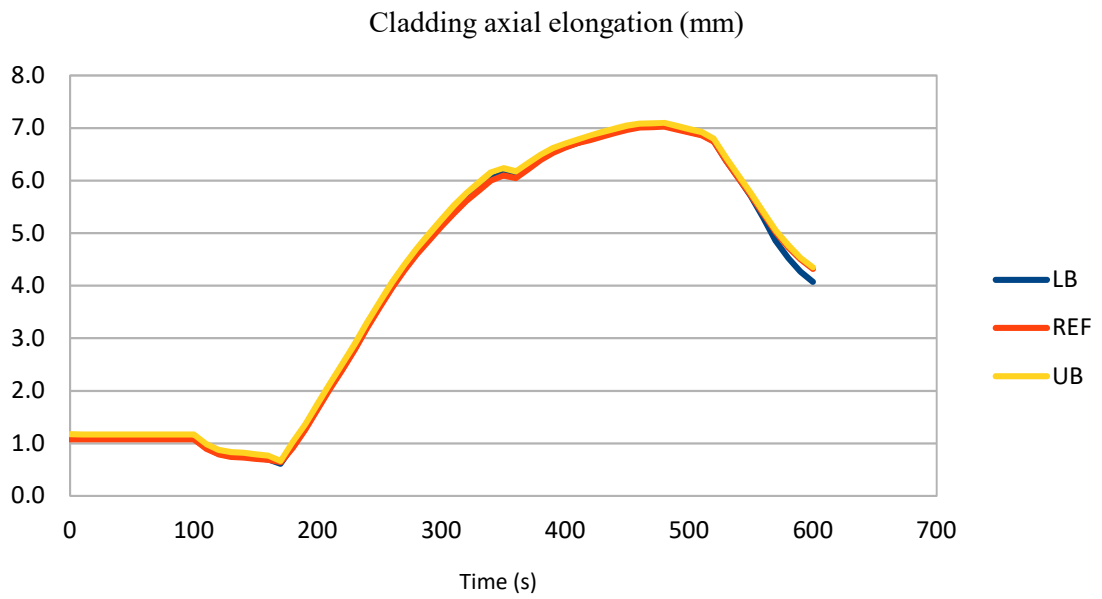


FIG. 27. Cladding (stainless steel) axial elongation profile during the transient.

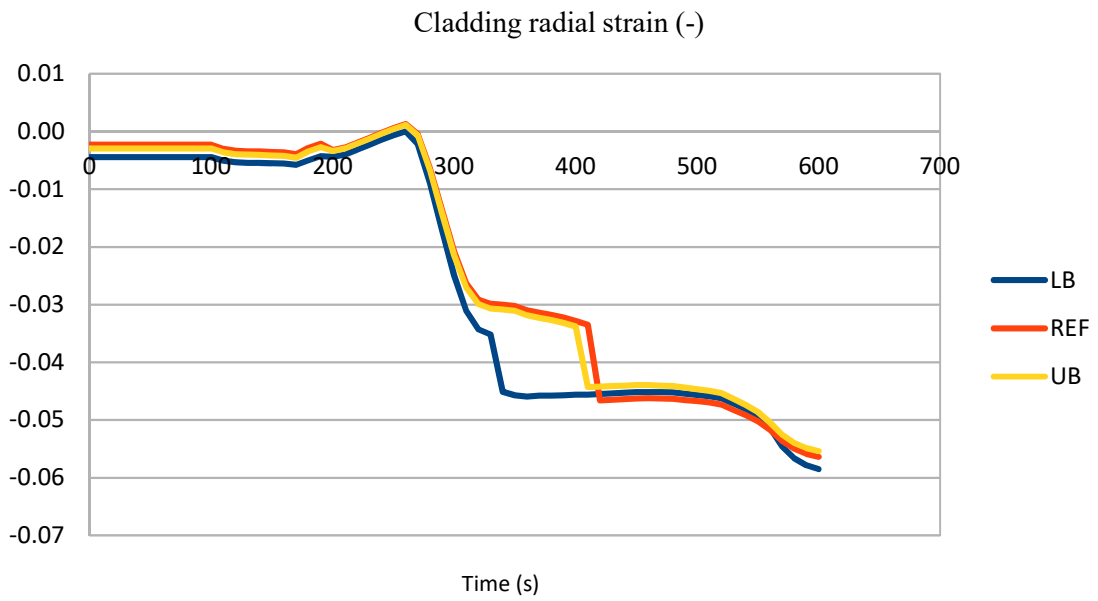


FIG. 28. Cladding (stainless steel) radial strain profile during the transient.

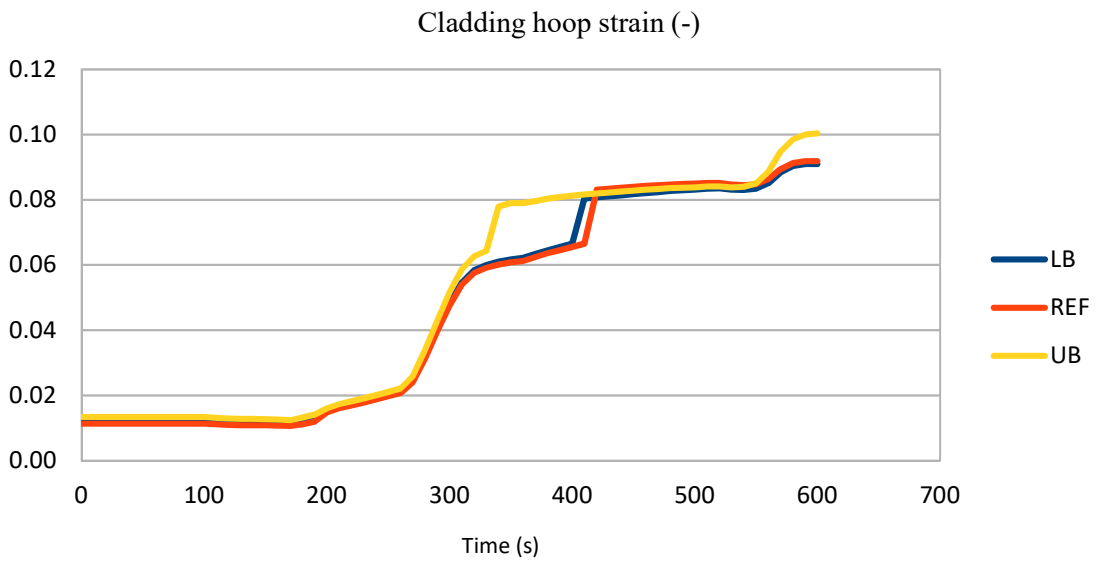


FIG. 29. Cladding (stainless steel) hoop strain profile during the transient.



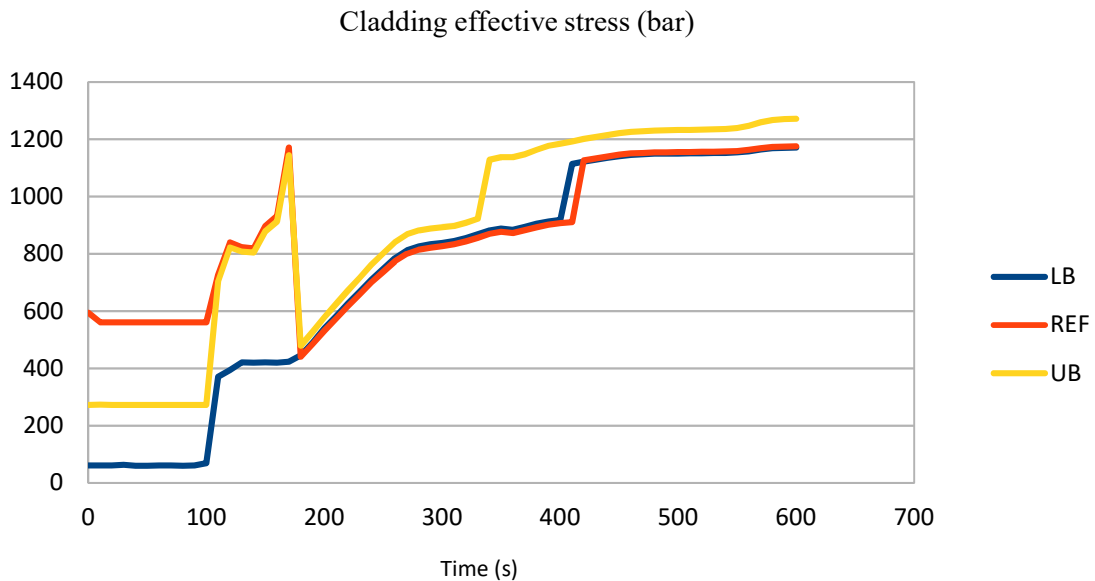


FIG. 30. Cladding (stainless steel) effective stress profile during the transient.

### 3. ANALYSIS AND CONCLUSIONS

One of the challenging design basis accidents for water cooled reactors is the loss of coolant (LOCA) caused by the failure of a large coolant pipe. More specifically, for the PWR reactor the initiating event of the design basis accident is the double-ended guillotine break of one of the large coolant pipes between the reactor vessel and the main circulation pump. In order to mitigate the consequences of this event, it is mandatory that all reactors must have an emergency core cooling systems in order to keep the fuel cooled efficiently and a coolable geometry through all phases of the accident. The requirement associated to coolable geometry and structural integrity is very challenging issue for fuel rod with zirconium alloy as cladding.

In the LOCA event there are at least two ways in that coolable geometry of the reactor core could be compromised: fuel clad ballooning which can lead to partial blockage of the fuel assembly channel and loss of cladding integrity during the emergency cooling system actuation (quench and loading associated after quench). The U.S. NRC (American Nuclear Regulatory Commission) address the issue considering requirement for peak cladding temperature (PCT < 1204°C) and a maximum cladding oxidation of ECR < 17%.

Before discussing the criteria associated to coolability and their implication is important to review some aspects of Zircaloy as fuel cladding material. During the sixties (1960's), zircaloy became the standard material for cladding materials in Light Water Reactors (LWR), Zircaloy-2 in BWR cores and Zircaloy-4 in PWR cores. However, besides the fuel assemblies, most of the structural components remained to be made from stainless steel or Ni-alloys. Later, the use of zircaloy for other fuel components occurred mainly after the eighties (1980s). Due to corrosion detected in the current zircaloy, an optimized Zircaloy-4 was developed at Siemens named PCA-Zircaloy (with PCA for 'Prime Candidate Alloy') mainly for PWR reactor and other designers/vendors were following with improved Zircaloy-4 cladding material, such as: AFA 2G-Cladding by Framatome/Fragema, OPTINTM by ABB and "Improved Zircaloy-4" from Westinghouse.

The improvement knowledge obtained during the optimization of zircaloy gives a new generation of zirconium material cladding for PWR, called "Duplex Cladding". Others different composition were made available in order to increase the corrosion resistance, such as M5, M4, HPA-4 (Siemens), ZIRLO (Westinghouse), HANA (KNFC), E635 and E110(Russia). These are the alloys currently utilized and some of them have substantial operational experience in

commercial PWRs and performance data from experiments (in-pile tests) performed under operational and accident condition.

Nowadays, the new alloys mentioned above are currently utilized and level of burnup increase compared at a time when the acceptance criteria was established. The aim of the criteria was to ensure some margin of ductility would remain in the zircaloy cladding when subject to quench process and therefore the reactor core could remain essentially intact and keep some condition for long term cooling. Furthermore, such criteria (PCT and ECR) include some conservatism degree due to lack of data related to oxidation embrittlement. Later, in 1988 the NRC considered that there are sufficient experimental data to quantify the degree of conservatism associated to the current criteria and amended the requirements of 10CFR50.46 Appendix K for the use of best-estimate models, including the Cathcart-Pawel oxidation correlation, therefore somehow these regulations would reflect the improved understanding of the phenomena that occurs during the LOCA transient.

Currently, many experimental data have shown that different factors can influence cladding embrittlement during a LOCA event; several important variables can influence and contributes including initial pre-transient hydrogen content, breakaway oxidation, inner surface oxygen uptake. Moreover, some others contribution are not clearly well-understood.

The CRP FUMAC was an excellent opportunity to address and verify how existing fuel performance code can simulate properly the LOCA event considering experiment performed specifically for LOCA evaluation, such as IFA-650 experiments series, CORA from KIT, NRC-STUDVIK and others.

Moreover, verify the sensitivity and uncertainties related to fuel parameters (fabrication, models, boundary condition, etc.) that could affect and/or have some correlation to the fuel cladding integrity.

The objective proposed by IPEN/CNEN (Brazil) was accomplished considering the investigation performed using stainless steel as cladding. The most important outcome of the CRP-FUMAC participation is the performance of stainless steel during the accident of loss of coolant, the fuel cladding integrity was preserved during all steps of the LOCA event, furthermore after Fukushima accident and all research related to ATF fuel, the iron based alloy can be a very promising candidate, especially stainless steel.

## REFERENCES

- [1] PARSONS, P.D., HINDLE, E.D., MANN, C.A., “PWR Fuel Behaviour in Design Basis Accident Conditions. A State-of-the-Art Report by the Task Group on Fuel Behaviour of CSNI Principal Working Group No 2”, Committee on the Safety of Nuclear Installations, OECD-NEA, NEA/CSNI-129, (1986).
- [2] U.S. NUCLEAR REGULATORY COMMISSION, “Acceptance Criteria for Emergency Core Cooling Systems for Light-Water Nuclear Power Reactors”, 10 CFR 50.46, USA.
- [3] CHUNG, H.M. “Fuel Behavior under Loss-of-Coolant-Accident Situations”, Nucl. Eng. Technol. , Vol. 37, 327 (2005).
- [4] HESSON, J.C. et al., Laboratory Simulations of Cladding-Steam Reactions Following Loss-of-Coolant Accidents in Water-Cooled Power Reactors, Argonne National Laboratory, ANL-7609 (1970).
- [5] MASSIH, A.R., Transformation Kinetics of Zirconium Alloys under Non-Isothermal Conditions, J. Nucl. Mater., Vol. 384, (2009) 330–335.
- [6] NAGASE, F., FUKETA, T., Investigation of Hydride Rim Effect on Failure of Zircaloy-4 Cladding with Tube Burst Test. J. Nucl. Sci. Technol., Vol. 42, (2005) 58.
- [7] UDAGAWA, Y., NAGASE, F., FUKETA, T., Effect of Cooling History on Cladding Ductility under LOCA Conditions, J. Nucl. Sci. Technol., Vol. 43, (2006) 844.

- [8] M. Ek, “LOCA Testing at Halden, the Third Experiment IFA-650.3”, OECD Halden Reactor Project, HWR-785, (2005).
- [9] MANNGARD, T., STENGARD, J., Evaluation of the Halden IFA-650 Loss-of-Coolant Accident Experiments 5, 6 and 7, 2014:19 ISSN:2000–0456, Swedish Radiation Safety Authority, Sweden (2014).
- [10] GEELHOOD, K. J., LUSCHER, W.G., FRAPCON-3.5: A Computer Code for the Calculation of Steady-State, Thermal-Mechanical Behavior of Oxide Fuel Rods for High Burnup, Vol. 1, Rev.1, NUREG/CR-7022, (2014).
- [11] GEELHOOD, K. J., LUSCHER, W.G., CUTA. J. M., FRAPTRAN-1.5: A Computer Code for the Transient Analysis of Oxide Fuel Rods, Vol. 1 Rev.1, NUREG/CR-7023, U.S. Nuclear Regulatory Commission (2014).
- [12] KULA, A., GIOVEDI, C., TEIXEIRA, A., GOMES, D.S., Revisiting Stainless Steel as PWR Fuel Rod Cladding after Fukushima Daiichi Accident, J. Energ. Eng., Vol. 8, (2014) 973–980.
- [13] MASSEY, C.P., TERRANI, K.A., DRYEPONDT, S.N., PINT, B.A., J. Nucl. Mater., 470, (2016) 128–138.
- [14] HAGRMAN, D.L., “Code Development and Analysis Program Cladding Mechanical Limits (CMLIMIT)”, Report prepared by EG&G - IDAHO CDAP-TR-056.
- [15] DESU, R. K., et al., “Mechanical Properties of Austenitic Stainless Steel 304L and 316L at Elevated Temperatures,” J. Mater. Res. Technol., 5, (2016) 13–20.